CONFERENCE PRE-PRINT
SYSTEMS INTEGRATION / FUSION ENERGY TECHNOLOGY (TEC)

A NOVEL MULTI-TIMESCALE STRATEGY FOR FUSION SYSTEMS CODES AND ITS IMPACT TO FUSION POWER PLANTS PARAMETRIC ANALYSES

T. POMELLA LOBO
Karlsruhe Institute of Technology (KIT)
Karlsruhe, Germany
Email: t.pomella-lobo@outlook.com

I.A. MAIONE
Karlsruhe Institute of Technology (KIT)
Karlsruhe, Germany

Abstract

Fusion Systems Codes (SCs) are fundamental tools that allow for parameter space exploration and evaluation of technology integration through parametric analyses that may identify relevant systemic dependencies in Fusion Power Plants (FPPs). However, current state-of-the-art SCs model each plant system operating within its own inherent timescale, and neglect the dynamic interdependence between them at a power plant level. The goal of this work is to illustrate this need for Multi-Timescale (MT) SCs with novel parametric dependencies, such as between the ejection velocity of plasma filaments to the Scrape-Off Layer (SOL) and the net power production of the plant, or between the design temperature of the FW and aspects of tritium self-sufficiency. For that, a novel strategy to produce MT SCs was tested with a EU-DEMO model built in MIRA, a multi-fidelity SC developed at the Karlsruhe Institute of Technology. This strategy identified three timescales in which most FPP systems are categorized: **(a)** the characteristic time in which *Plasma* dynamics evolve, **(b)** a single reactor *Pulse* and **(c)** the *Operation* of a FPP (a collection of pulses). New models have been developed to depict essential phenomena of systems in each timescale. For **(c)**, a multi-species Fuel Cycle module (FCM) computes fuel accumulation rates using a residence-times (τ) model, with τ-parameters derived from the characterization of selected technologies. For **(b)**, a Power Cycle module (PCM) computes the net power production by the Balance-of-Plant systems using thermodynamic models. For **(a)**, SOL plasma dynamics are computed with scaling laws and an optimized surrogate of the code TOKES, to estimate heat and particle distributions along the reactor chamber wall. Consistent coupling is ensured by using results from (**c**) to compute outgassing fluxes with the double-diffusion code TESSIM-X. This impacts the dwell-time, and thus the dynamics of both (**a**) and (**b**), and leads to stronger dependencies than those obtained from non-MT analyses.

Keywords: Scrape-Off Layer (SOL), Balance-of-Plant (BOP), Fuel Cycle, Systems Code, EU-DEMO

1. INTRODUCTION & BACKGROUND

Systems Code are fundamental tools in Fusion Energy research that allow for parameter space exploration and evaluation of technology integration through parametric studies [1]. Many Fusion Systems Codes (FSCs) focus on reactor design to identify relevant systemic dependencies, and a few target design of Fusion Power Plants (FPPs) (*e.g.* [2–6]). However, current state-of-the-art SCs of the latter type model each plant system operating within its own inherent timescale and neglect the dynamic interdependence between them at the power plant level. That is, these implementations can be arguably classified as Reactor Design Codes (RDCs), some with post-processing modules for auxiliary plant systems, instead of true Plant Design Codes (PDCs). The development of PDCs could be used to study, for example, how the length of the dwell-time may impact the dynamics of both the power and fuel balances of a FPP (*e.g.* [7, 8]). Instead of a fixed assumption for the time of dwell, *e.g.* 10 min, the calculation of the Central Solenoid (CS) recharge and pump-down times, consistent with reactor design, could be coupled with Balance-of-Plant (BOP) and Tritium Plant (TP) models. Preliminary analyses show that such studies may

reveal unexpected parametric dependencies never reported in literature. Examples include dependencies between the ejection velocity of plasma filaments to the Scrape-Off Layer (SOL) and the net power production of the plant, or between the design temperature of the First Wall (FW) and aspects of tritium self-sufficiency.

In other words, Multi-Timescale (MT) FSCs are needed. To fill out this gap, the development of a strategy to convert current RDCs into PDCs has been proposed as part of a multi-year project [9–12], which could potentially increase the utility of codes already available. Candidate strategies can be tested on an existing RDC, and representative parametric analyses of an FPP concept can be used to illustrate the importance of pivoting current FSCs into PDCs. A promising candidate foresees the introduction of a methodology to categorize FPP systems in one of three timescales relevant for MT analyses, as shown in Figure 1. The **(a)** *Plasma* timescale represents the characteristic time in which plasma dynamics evolve [13], which is crucial to characterize the reactor. The **(b)** *Pulse* timescale is inherent to tokamak design and mainly impacts the net power production of the plant [14]. The **(c)** *Operational* timescale comprises in collections of pulses and majorly impacts fuel self-sufficiency and availability of a FPP [15].

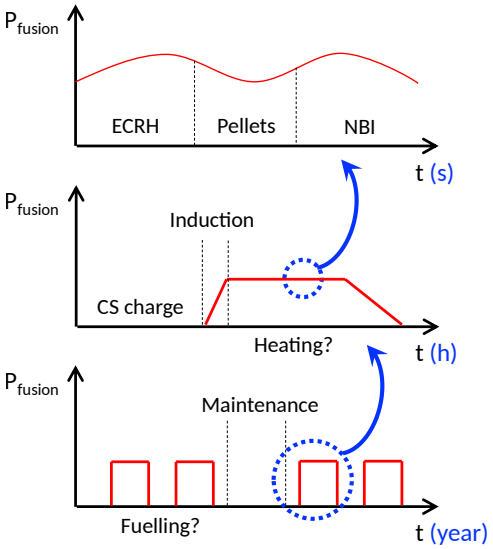

FIG. 1. Schematic view of fusion power production in a tokamak-based FPP in different timescales (*top* to *bottom*: plasma, pulse, operation) and the potential impact of different plant systems.

Following work previously done at the Karlsruhe Institute of Technology (KIT), the multi-fidelity MIRA code [16] has been chosen to test this candidate strategy. Converting MIRA into a PDC requires adapting some of its existing models as well as developing new ones. Its Reactor module (RCM) includes a coils characterization model that is able to estimate the CS recharge time, but a zero-dimensional (0D) model for the SOL physics that neglects (power and mass) fluxes due to charged particles on the FW. This prevents the calculation of outgassing from chamber walls during the dwell, which is arguably the effect that dominates pumping dynamics and determines the time required for pump-down (Δt_{PD}) [17]. Its BOP model is based on conversion efficiencies only, and lacks a thermodynamic framework to enable estimation of transient effects. No TP model is currently present. For these reasons, the following steps are required:

- the implementation of new transport models in the RCM to represent **(a)**, for particles both in the SOL (for the calculation of chamber wall loading by plasma particles), and in condensed matter (for the outgassing of those walls);
- the development of a Power Cycle module (PCM) to represent **(b)**, for the calculation of power and mass balances in the BOP and other systems associated with electricity production;
- and the development of a Fuel Cycle module (FCM) to represent **(c)**, for the calculation of mass balances in the TP and other systems associated with fuel (*i.e.* tritium) production.

A final Time Control module (TCM) is also foreseen to couple all three timescales and enable plant-wide systems-level analyses. The goal of this work is to describe the modeling approach applied for the first, and report on preliminary results of the RCM for Δt_{PD}. The simulations presented here refer to the Helium-Cooled Pebble Bed (HCPB) variant of the European DEMOnstration Power Plant, 2017 Baseline (EU-DEMO), with an indirect BOP.

2. METHODOLOGY TO COMPUTE Δt_{PD}

The new transport models developed for the RCM allow a FSC to estimate the Δt_{PD}. To that end, particle fluxes into the chamber walls during the flat-top must be computed, to allow for a subsequent calculation of the effusion fluxes out of the same walls during dwell. Modeling of SOL heat fluxes can be used to estimate their associated particle fluxes, so Subsection 2.1 presents the methodology to calculate both using the results of a confined plasma equilibrium and transport code, such as MIRA enhanced with PLASMOD [18]. Subsection 2.2 then presents how these fluxes are subsequently applied in a code to compute double-population transport of hydrogen isotopes in metals (TESSIM-X), to estimate wall effusion, and the resulting pump-down dynamics.

2.1. Modeling SOL fluxes

Figure 2 depicts a recurring systemic approach applied in literature to estimate heat fluxes in the SOL and their deposition on different systems that interface with the plasma [19, 20]. It relies on a steady-state representation of the transport and power balance between the confined plasma and the regions between the separatrix and the walls. The balance is computed for different contributions crossing the separatrix: carried by neutrons ($\tilde{\Psi}_n^{sep}$), photons ($\tilde{\Psi}_\gamma^{sep}$) and charged particles ($\tilde{\Psi}_q^{sep}$). Neutronic power presents mostly volumetric deposition, and is thus a concern for Breeding Zone (BZ) and Divertor Cassette (DC) design. Photonic power presents superficial deposition, but its distribution is mostly isotropic and altered by source distribution in the confined region. Charged particles power is the one most impacted by SOL dynamics, and is generally sub-divided into three channels after experimental observation of two main deposition regions: the Near-SOL (NS) and the Far-SOL (FS).

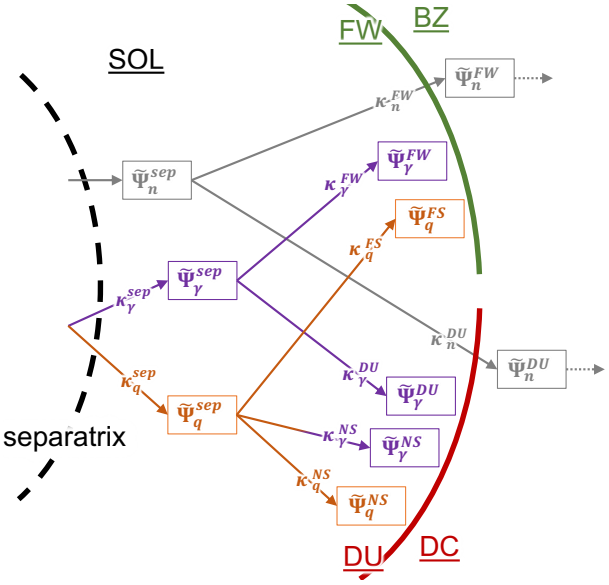

FIG. 2. Diagram of the steady-state power balance and distribution between Scrape-Off Layer (*left*) and deposition on wall systems (*right*). Power crossing the separatrix (*dashed black curve*) is carried by neutrons (*grey boxes*), photons (*purple boxes*) or charged particles (*orange boxes*). Deposition starts at the First Wall (FW) (*green curve*) and at the Divertor (Plasma-Facing) Units (DU) (*red curve*), and extends to further components beyond.

Power deposited in the NS is mainly attributed to confined particles diffusing through the separatrix and following magnetic field lines until encountering any reactor wall segment. These carry a significant portion of the charged particle power and end in a relatively narrow portion of the chamber walls. To comply with technological constraints such as the Divertor (DV) challenge coefficient, impurity seeding is usually assumed necessary, to convert part of the power carried by these particles into an additional radiative contribution ($\tilde{\Psi}_\gamma^{NS}$), and reduce the actual power carried by charged particles ($\tilde{\Psi}_q^{NS}$) [21]. Power deposited in the FS ($\tilde{\Psi}_q^{FS}$), on the other hand, is generally attributed to turbulent processes in the confined region, predominantly the ejection of "blobs". Such plasma filaments are coherent structures created within the confined region that propagate into and across the SOL due to $\vec{E} \wedge \vec{B}$ drift, deforming along the way. Their transport is considered the main culprit of power deposition in the FW due to charged particles. And in fact, the turbulence that originates blobs can create large density fluctuations, which means that the blob population can contain significant fractions of the total flow of particle exiting confinement [22].

Characterization of NS heat fluxes is usually achieved with empirical laws such as the Eich scaling [23, 24]. The expression dependency with the radial distance (d) is measured from the separatrix up to the wall, at the reactor midplane. This distribution needs then to be mapped to the points of contact of the field lines with the walls, since the magnetic field is expanded there to reduce the $\tilde{\Gamma}_q^{NS}$ and comply with heat removal technological capabilities [25]. By assuming that all particles escaping confinement towards both SOL regions have the same average energy per particle, the total charged particle flow across the separatrix (Ψ_q^{sep}) can be split using the same coefficients applied to the heat distribution in the SOL. Furthermore, with the charged particle flow in the NS (Ψ_q^{NS}), the charged particle flux in the NS (Γ_q^{NS}) can be estimated by using the same dependency applied for the heat fluxes and field mapping between the midplane and chamber wall:

$$\Psi_q^{sep} = \frac{\Psi_q^{NS}}{\kappa_\gamma^{NS} + \kappa_q^{NS}} = \frac{\Psi_q^{NS}}{\kappa_q^{NS}} \tag{1}$$

$$\tilde{\Gamma}_q^{NS}(d) = \frac{\tilde{\Psi}_q^{NS}}{2 \cdot \pi \cdot R_p \cdot \lambda_{NS}} \cdot e^{-\frac{d}{\lambda_{NS}}} \quad \Longrightarrow \quad \Gamma_q^{NS}(d) = \frac{\Psi_q^{NS}}{2 \cdot \pi \cdot R_p \cdot \lambda_{NS}} \cdot e^{-\frac{d}{\lambda_{NS}}} \tag{2}$$

Characterization of FS heat fluxes, on the other hand, is a bigger challenge. Empirical laws for this region are notoriously difficult to be developed and validated [26] and first-principles modeling usually requires considerable computational power [27]. For these reasons, a dedicated study was previously performed to develop a surrogate model of the TOKES code, that applies a palliative approach by modeling plasma filaments with simplified fluid-dynamics. It achieves this computing the evolution of plasma parameters inside filaments after ejection, and re-normalizing the heat and particles deposition due to a single blob with respect to $\tilde{\Psi}_q^{FS}$ and Ψ_q^{NS}, assuming it an average representative of the blobs population [28]. The results of that study and its optimized surrogates can be found elsewhere [29].

2.2. Modeling chamber wall outgassing

Coupling of the diffusion trapping code TESSIM-X to MIRA allows for the calculation of effusion fluxes, in a similar manner to previous similar studies [8, 30]. The model is run for a loading phase equal to the flat-top duration, and diffusion is recorded for ∼2000 s after that. Pure gas loading is not considered; instead implantation of energetic ions is imposed on a first 2 mm tungsten layer adjacent to a second 10 mm iron layer, that represents EUROFER97. Implantation is modeled as a source term in the first layer, with a Gaussian distribution. Depth and standard deviation are quickly calculated for both deuteron and triton fluxes using logarithmic and polynomial curves fitted from results of the SDTrim.SP code (all statistic $R^2 > 99\,\%$). The same is done for reflection coefficients (both $R^2 > 92\,\%$). Diffusion parameters are taken from recent literature for tungsten [31] and EUROFER97 [32]. Trapping parameters are taken from models that consider irradiation, both for tungsten [33] as well as EUROFER97 [34, 35]. The mean energy of implantation ions is currently assumed 100 eV [36], while more precise models for recycling and charge exchange in the SOL are not implemented. The surface temperature is currently assumed 800 K, with gradients of $1\,\mathrm{K\,mm^{-1}}$ and $20\,\mathrm{K\,mm^{-1}}$ for each layer, but will be taken from the PCM in the future [12].

Different positions along the reactor chamber wall exhibit different particle fluxes, so TESSIM-X is run for multiple positions along the wall. Flux values are "sampled" from the complete poloidal profile of particle fluxes, in such a way that values are representative of the range of values computed by the SOL transport model(s). This is done with an adaptive Cumulative Distribution Function (CDF) implementation that separates particle fluxes in (logarithmically-spread) bins, and increases sampling probability in profile sections that have flux values more frequently registered in the profile. Since each flux value must be applied in a separate simulation, TESSIM-X is coupled to MIRA as to enable parallel computation, in the interest of speed. Each simulation provides effusion fluxes from the wall during the dwell period, as a function of time. The results of all simulations are collected to build an interpolation model that enables the estimation of effusion fluxes on all positions along the wall. Since effusion exhibits logarithmic dependency with multiple parameters, the interpolation model is built on the logarithm of simulation results. The interpolation model is then applied to compute a toroidal integral and determine the total effusion flow due to outgassing (Ψ_{out}) from the complete reaction chamber. Integration is repeated for each time step, and applied with the spline method to reduce numerical errors induced by the interpolation.

This effusion flow in function of time can then be utilized to estimate the time required for pump-down (Δt_{PD}) by evolving the equation:

$$V \cdot \frac{d}{dt} p + S_{pump} \cdot p = \Psi_{out}(t) \tag{3}$$

dependent on the chamber volume (V) and the effective pumping speed (S_{pump}). The former is computed by toroidal revolution of the chamber wall cross-section area, while the latter is currently assumed $100\,\mathrm{m^3\,s^{-1}}$. Chamber pressure ($p$) during the dwell is assumed to start at 1 Pa, and the target to be reached before a new pulse is set at 5×10^{-4} Pa [17]. The full pressure

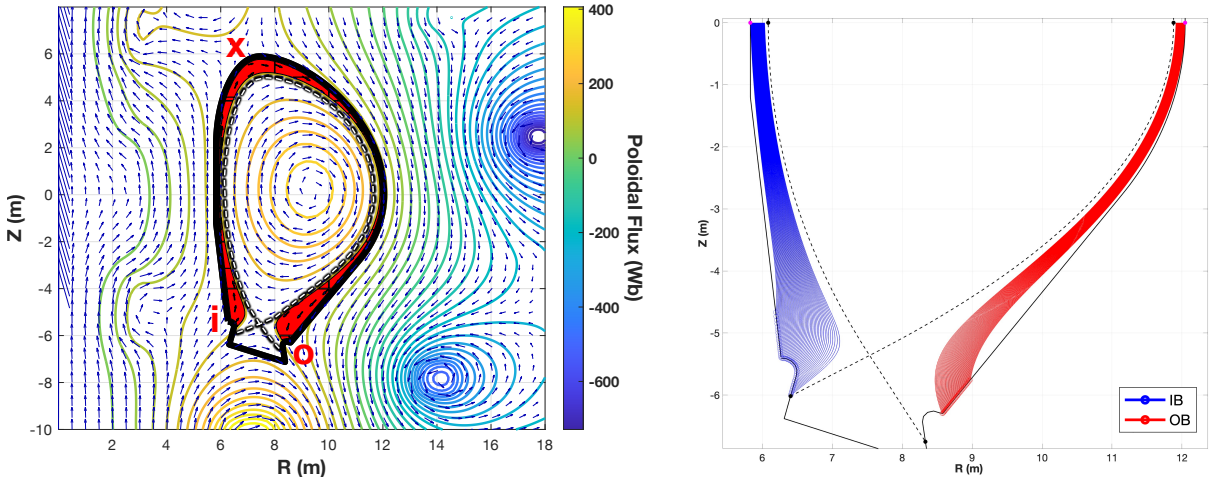

(a) Magnetic field (*blue arrows*) and poloidal flux surfaces (*coloured lines*). Transport phenomena of interest occur in the SOL (*red region*, approximated). Letter labels (in *red*) indicate points of interest along the walls: lowest inboard (*i*) and outboard (*o*) points, as well as the wall point closest to the upper (ex-vessel) X-point in the magnetic saddle (*x*).

(b) Visualization of the paths taken by midplane particles diffusing in the NS, projected onto a 2D tokamak cross-section. Paths calculated at both inboard (*blue*) and outboard (*red*) of the reactor are limited by grid precision, which explains the space unfilled by streamlines between the separatrix and the colored paths.

FIG. 3. Magnetic configuration in a flat-top snapshot computed by MIRA, depicting the separatrix (*dashed line*) and chamber walls (*black curve*), and the resulting paths that determine Near-SOL (NS) wall deposition profiles.

evolution in time is recorded to also fit an exponential dependency, in such a way that a pump-down characteristic time (τ_{PD}) may also be computed. This is intended to later couple these dynamics with the FCM [9].

3. PRELIMINARY Δt_{PD} RESULTS AND DISCUSSIONS

3.1. Heat and particle fluxes in the SOL due to charged particles

Figure 3 illustrates the methodology presented in Subsection 2.1 to estimate the NS heat and particle flux deposition profiles on the reactor chamber walls. Figure 3a depicts the the magnetic field, poloidal flux and chamber wall maps produced by MIRA, that are the starting data for applying the new SOL model. Walls are represented by a single contour, although different segments belong to different systems. Assuming an axyssymetric 2D representation, Limiters (LMs) are neglected and only the Breeding Blanket (BB) and the DV are depicted. In counter-clock direction: the DU is defined between the lowest inboard (*i*) and outboard points (*o*); the FW is defined in its complement, passing though the segment closest to the upper X-point (*x*).

The same contour can be seen in Figure 3b, which also shows the flight-paths calculated for test particles starting at the mid-plane level ($Z = 0$) until they reach the walls. These paths are only a 2D projection on the $R \times Z$ plane, and hide the fact that particles also travel in the toroidal direction, roughly at a ratio determined by the safety factor ($q_s(r) = {}^{r \cdot B_t(r)}/_{R \cdot B_p(r)}$). The streamlines associate points at the mid-plane with points at the wall, which defines a mapping for the deposition of NS heat and particle fluxes. Lines starting close to the separatrix at the mid-plane connect to points close to the separatrix strike-points on the wall (*black dots*). The points of connection of lines are spaced farther apart on the wall then their starting points on the mid-plane. This implies that the exponential distributions for heat and particles given in Equation 2 become spread onto segments of larger width, which is captured by the model. This translates into larger surface areas in the full 3D toroidal geometry, reducing fluxes at the walls. However, the first 20 % of the mid-plane space between the separatrix and the walls are skipped in the calculation of streamlines because of the limited precision of the magnetic grid applied in the construction of the NS and FS models. This limitation reduces the resolution of the calculated fluxes, and is a known challenge for simplified SOL models [25]. It can be potentially improved with a refinement of the mesh built by MIRA's magnetic equilibrium model, but the current results are not considered detrimental in the framework of FSCs because of their goal of (fast) systemic analyses, instead of (computationally intensive) dedicated wall design.

The success of the model is further demonstrated by the superposition of NS and FS deposition profiles, shown in Figure 4. The profiles depict both heat and particle fluxes along a wall coordinate measured in the counter-clockwise direction, starting at the lowest inboard point (label *i* in Fig. 3a). The figure focuses on the highest flux values of both profiles to increase visibility, so lowest values are not represented, such as the lack of deposition in the private area of the DV (region between 0 m to 5 m) due to the NS transport model neglecting collisions. The highest deposition values are observed close to the separatrix strike-points, including heat fluxes between 1 MW m^{-2} to 10 MW m^{-2}. Values are compatible with the estimates produced

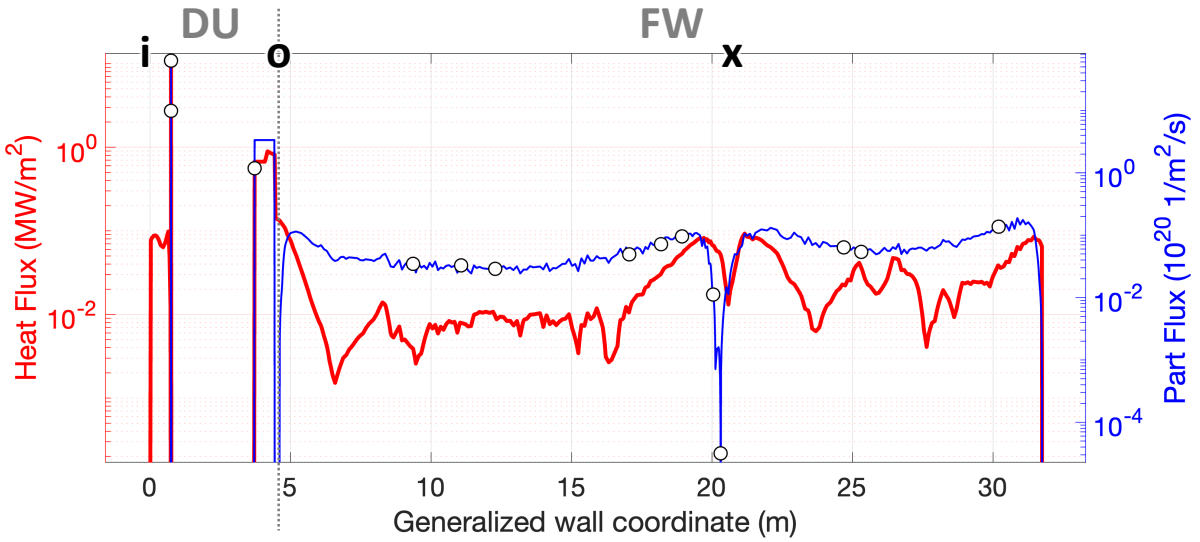

FIG. 4. Superposition of NS and FS poloidal profiles for both heat (*red*) and particle (*blue*) fluxes. The same labels (*black letters*) as seen in Fig. 3a are used to distinguish wall sections of the DU and FW. Profiles are measured along a generalized wall coordinate that rotates in counter-clockwise direction, starting at the lowest inboard point. Representative values of the particle flux profile (*white circles*) are obtained through an adaptive CDF sampling approach (*vide* Subsec. 2.2) and are used to run TESSIM-X and characterize the effusion flow during pump-down.

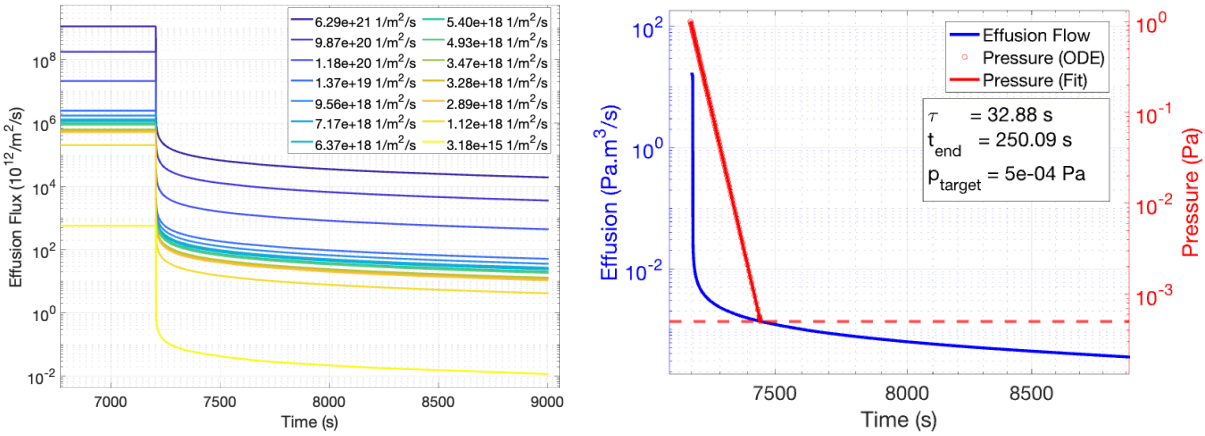

(a) Outgasssing (un-loading) effusion fluxes simulated by TESSIM-X for different (loading) particle fluxes sampled along the wall (*vide* Fig. 4), ordered by magnitude.

(b) Effusion flow (*blue*) obtained through toroidal integration of the effusion fluxes model produced with the results shown in Fig. 5a, and subsequent pump-down dynamics (*red*).

FIG. 5. Results of TESSIM-X simulations and subsequent calculation of pump-down dynamics.

by the previous 0D model of MIRA for the SOL, that enforced a heat flux in the DV targets of $10\,\mathrm{MW\,m^{-2}}$ to calculate the required argon seeding for detachment regime [18]. However, the new model overestimates the heat flux at the inboard because of the narrow width of the deposition region for the first $20\,\%$ of the power distribution (*i.e.* due to the low resolution of the magnetic grid, *vide* above). For wall coordinates above $5\,\mathrm{m}$, all deposition values are predicted by the FS model. Power and mass balance checks performed independently in each SOL region verify conservation, so the combined profiles are considered sufficient to fully characterize the charged particle flows in the SOL.

3.2. Effusion fluxes and pump-down dynamics

Figure 5 shows the results of running fourteen (parallel) TESSIM-X simulations using the particle flux values sampled from the profiles of the SOL model, and their subsequent use in calculating the pump-down dynamics. Samples include extremes of the range of values that the particle fluxes assume, after neglecting null fluxes (not depicted in the logarithmic scale applied in Fig. 4). The adaptive CDF algorithm is able to properly distribute sampling across the profile, but increases the density of sampling around most common values (*i.e.* peaks and vales exhibit fewer samples than plateaus). Figure 5a shows the outcome of the outgassing simulated by TESSIM-X for each sample. As expected, high (loading) particle fluxes lead to high (un-loading) effusion fluxes from the wall. Similarly, low profile values lead to low effusion, with a roughly logarithmic progression between model inputs and outputs. This suggests the logarithmic-interpolation approach is sufficient to estimate the results of TESSIM-X for wall points between samples.

Figure 5b shows the total effusion flow expected in the reactor chamber after toroidal integration of the effusion fluxes estimated by the logarithmic-interpolation model. The flow is converted to (Normal) $\mathrm{Pa\,m^3\,s^{-1}}$ to match literature on tokamak pumping technologies. The pump-down dynamics are evolved (*vide* Eq. 3) until the target pressure is reached, and the time since the start of dwell (t_{end}) is measured to determine the minimum time needed between pulses to evacuated the chamber (*i.e.* Δt_{PD}). Results match current literature expectations for walls in pristine (*i.e.* un-damaged) conditions [37]. The exponential fit to the evolution of the pressure decrease provides the characteristic time marked as τ (in other words, τ_{PD}), for future coupling with a fuel balance model. Both results indicate the methodology proposed is a viable approach to introduce an estimate of the pump-down dynamics into a FSC.

4. OUTLOOK

The methodology introduced in this work is demonstrated to be sufficient for producing systemic analyses in the framework of FSCs. With the new model at hand, parametric analyses are under way to identify relevant dependencies between technological aspects of different FPP systems. To that end, the following steps are foreseen in the fully coupled code:

- implement a simplified materials model to modify the inputs provided to TESSIM-X and also represent damaged conditions for the walls, instead of only pristine conditions;
- forward Δt_{PD} to the transient thermodynamic model of the PCM, and retrieve the wall temperatures calculated for the FW to modify the inputs for TESSIM-X simulations;
- forward Δt_{PD} and τ_{PD} to the transient fuel balance model of the FCM and estimate impact to fuel (tritium) economics.

Figure 6 shows a preliminary parametric study using the FCM when applying trapping parameters that represent more realistic conditions for the reactor chamber walls. It confronts the tritium accumulation rate in the fuel storage of the TP when assuming a 10 min dwell period, against the rate expected for a 15 min dwell period. The foreseen implication is a lower accumulation rate, which implies in longer doubling times, among other consequences. The fully coupled code is expected to be applied to perform numerous such studies and reveal design-relevant dependencies through extensive sensitivity analyses.

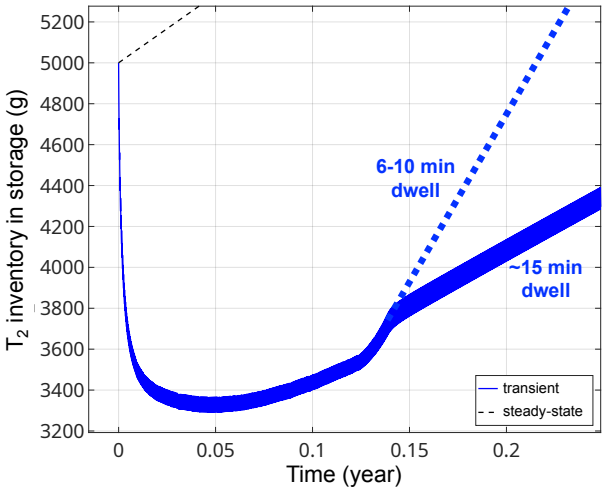

FIG. 6. Tritium accumulation in storage as a function of operational time of a FPP. Comparison between asymptotic accumulation rates of: steady-state model (*black dashed line*), transient model decoupled from systems modeled in other timescales (*blue dotted line*), and transient model run using the MT candidate strategy (*blue continuous line*).

ACKNOWLEDGEMENTS

The authors thank Klaus Schmid from the Max Planck Institute for Plasma Physics (IPP) for his invaluable support and counseling with the use of their TESSIM-X code.

This work has been carried out within the framework of the EUROfusion Consortium, funded by the European Union via the Euratom Research and Training Programme (Grant Agreement No 101052200 EUROfusion). Views and opinions expressed are however those of the author(s) only and do not necessarily reflect those of the European Union or the European Commission. Neither the European Union nor the European Commission can be held responsible for them.

REFERENCES

[1] Makoto Nakamura et al. "Efforts towards improvement of systems codes for the Broader Approach DEMO design". en. In: *Fusion Engineering and Design* 87.5-6 (Aug. 2012), pp. 864–867. ISSN: 09203796. DOI: 10.1016/j.fusengdes.2012.02.034. URL: https://linkinghub.elsevier.com/retrieve/pii/S0920379612000944 (visited on 10/16/2020).

[2] Lane Carlson et al. "ARIES systems code development, visualization and application". In: *2011 IEEE/NPSS 24th Symposium on Fusion Engineering*. Chicago, IL, USA: IEEE, June 2011, pp. 1–6. ISBN: 978-1-4577-0669-1. DOI: 10.1109/SOFE.2011.6052294. URL: http://ieeexplore.ieee.org/document/6052294/ (visited on 11/19/2024).

[3] M. Kovari et al. ""PROCESS": A systems code for fusion power plants - Part 1: Physics". en. In: *Fusion Engineering and Design* 89.12 (Dec. 2014), pp. 3054–3069. ISSN: 09203796. DOI: 10.1016/j.fusengdes.2014.09.018. URL: https://linkinghub.elsevier.com/retrieve/pii/S0920379614005961 (visited on 11/05/2019).

[4] C. Reux et al. "DEMO reactor design using the new modular system code SYCOMORE". In: *Nuclear Fusion* 55.7 (July 2015), p. 073011. ISSN: 0029-5515, 1741-4326. DOI: 10.1088/0029-5515/55/7/073011.

[5] M. Kovari et al. ""PROCESS": A systems code for fusion power plants – Part 2: Engineering". en. In: *Fusion Engineering and Design* 104 (Mar. 2016), pp. 9–20. ISSN: 09203796. DOI: 10.1016/j.fusengdes.2016.01.007. URL: https://linkinghub.elsevier.com/retrieve/pii/S0920379616300072 (visited on 02/11/2021).

[6] M. Coleman and S. McIntosh. "BLUEPRINT: A novel approach to fusion reactor design". en. In: *Fusion Engineering and Design* 139 (Feb. 2019), pp. 26–38. ISSN: 09203796. DOI: 10.1016/j.fusengdes.2018.12.036. URL: https://linkinghub.elsevier.com/retrieve/pii/S0920379618308019 (visited on 10/16/2020).

[7] Salvatore D'Amico et al. "Preliminary thermal-hydraulic analysis of the EU-DEMO Helium-Cooled Pebble Bed fusion reactor by using the RELAP5-3D system code". en. In: *Fusion Engineering and Design* 162 (Jan. 2021), p. 112111. ISSN: 09203796. DOI: 10.1016/j.fusengdes.2020.112111. URL: https://linkinghub.elsevier.com/retrieve/pii/S0920379620306591 (visited on 10/07/2021).

[8] K. Schmid et al. "Implications of T loss in first wall armor and structural materials on T-self-sufficiency in future burning fusion devices". In: *Nuclear Fusion* 64.7 (July 2024), p. 076056. ISSN: 0029-5515, 1741-4326. DOI: 10.1088/1741-4326/ad52a7. URL: https://iopscience.iop.org/article/10.1088/1741-4326/ad52a7 (visited on 07/03/2024).

[9] Tiago Pomella Lobo et al. *A Time-Dependent Fuel Cycle developed for Multi-Timescale Systems-Codes to study technology integration in advanced Fusion Power Plants*. Poster. virtual edition, Sept. 2020. URL: https://soft2020.eu/.

[10] Tiago Pomella Lobo, Ivan A. Maione, and Lorenzo V. Boccaccini. *A Time-Dependent Power Cycle developed for Multi-Timescale Systems Codes to study technology integration in advanced Fusion Power Plants*. Poster. Dubrovnik, Croatia, Sept. 2022. URL: https://soft2022.eu/.

[11] Tiago Pomella Lobo, Sergey Peschanyy, and Ivan A. Maione. *A Reduced-Order Model to Estimate First Wall Particle and Heat Fluxes for Systems Codes*. Poster. Las Palmas de Gran Canaria, Spain, Sept. 2023. URL: https://isfnt2023.com/.

[12] Tiago Pomella Lobo, Ivan A. Maione, and Alberto Ferro. *A Multi-Timescale approach for Fusion Power Plants Systems Codes focused on models for Fuel and Power Cycles*. Poster. Dublin City University, Ireland, Sept. 2024. URL: https://soft2024.eu/.

[13] Ehud Greenspan, ed. *Encyclopedia of nuclear energy*. English. OCLC: 1258649274. Amsterdam: Elsevier, 2021. ISBN: 978-0-12-819732-5. URL: https://search.ebscohost.com/login.aspx?direct=true&scope=site&db=nlebk&db=nlabk&AN=2720599 (visited on 07/28/2022).

[14] Simone Minucci et al. "Electrical Loads and Power Systems for the DEMO Nuclear Fusion Project". en. In: *Energies* 13.9 (May 2020), p. 2269. ISSN: 1996-1073. DOI: 10.3390/en13092269. URL: https://www.mdpi.com/1996-1073/13/9/2269 (visited on 03/09/2022).

[15] M. Coleman, Y. Hörstensmeyer, and F. Cismondi. "DEMO tritium fuel cycle: performance, parameter explorations, and design space constraints". en. In: *Fusion Engineering and Design* 141 (Apr. 2019), pp. 79–90. ISSN: 09203796. DOI: 10.1016/j.fusengdes.2019.01.150. URL: https://linkinghub.elsevier.com/retrieve/pii/S092037961930167X (visited on 10/23/2020).

[16] Fabrizio Franza. “Development and Validation of a Computational Tool for Fusion Reactors’ System Analysis”. de. PhD thesis. Karlsruher Institut für Technologie, 2019.

[17] Katharina Battes, Christian Day, and Volker Rohde. “Basic considerations on the pump-down time in the dwell phase of a pulsed fusion DEMO”. en. In: *Fusion Engineering and Design* 100 (Nov. 2015). Based on report: WPTFV–PR(15)01, pp. 431–435. ISSN: 09203796. DOI: 10.1016/j.fusengdes.2015.07.011. URL: https://linkinghub.elsevier.com/retrieve/pii/S0920379615302362 (visited on 05/12/2020).

[18] F. Franza et al. “MIRA: a multi-physics approach to designing a fusion power plant”. In: *Nuclear Fusion* 62.7 (July 2022), p. 076042. ISSN: 0029-5515, 1741-4326. DOI: 10.1088/1741-4326/ac6433. URL: https://iopscience.iop.org/article/10.1088/1741-4326/ac6433 (visited on 06/15/2022).

[19] R. Wenninger et al. “The DEMO wall load challenge”. In: *Nuclear Fusion* 57.4 (Apr. 2017), p. 046002. ISSN: 0029-5515, 1741-4326. DOI: 10.1088/1741-4326/aa4fb4. URL: https://iopscience.iop.org/article/10.1088/1741-4326/aa4fb4 (visited on 09/15/2021).

[20] F. Maviglia et al. “Impact of plasma-wall interaction and exhaust on the EU-DEMO design”. en. In: *Nuclear Materials and Energy* 26 (Mar. 2021), p. 100897. ISSN: 23521791. DOI: 10.1016/j.nme.2020.100897. URL: https://linkinghub.elsevier.com/retrieve/pii/S2352179120301587 (visited on 09/17/2021).

[21] G. Federici et al. “Relationship between magnetic field and tokamak size—a system engineering perspective and implications to fusion development”. In: *Nuclear Fusion* 64.3 (Mar. 2024), p. 036025. ISSN: 0029-5515, 1741-4326. DOI: 10.1088/1741-4326/ad2425. URL: https://iopscience.iop.org/article/10.1088/1741-4326/ad2425 (visited on 05/27/2025).

[22] D. A. D’Ippolito, J. R. Myra, and S. J. Zweben. “Convective transport by intermittent blob-filaments: Comparison of theory and experiment”. en. In: *Physics of Plasmas* 18.6 (June 2011), p. 060501. ISSN: 1070-664X, 1089-7674. DOI: 10.1063/1.3594609. URL: https://pubs.aip.org/pop/article/18/6/060501/387832/Convective-transport-by-intermittent-blob (visited on 02/14/2024).

[23] T. Eich et al. “Inter-ELM Power Decay Length for JET and ASDEX Upgrade: Measurement and Comparison with Heuristic Drift-Based Model”. en. In: *Physical Review Letters* 107.21 (Nov. 2011), p. 215001. ISSN: 0031-9007, 1079-7114. DOI: 10.1103/PhysRevLett.107.215001. URL: https://link.aps.org/doi/10.1103/PhysRevLett.107.215001 (visited on 09/25/2023).

[24] T. Eich et al. “Scaling of the tokamak near the scrape-off layer H-mode power width and implications for ITER”. In: *Nuclear Fusion* 53.9 (Sept. 2013), p. 093031. ISSN: 0029-5515, 1741-4326. DOI: 10.1088/0029-5515/53/9/093031. URL: https://iopscience.iop.org/article/10.1088/0029-5515/53/9/093031 (visited on 09/25/2023).

[25] F. Maviglia et al. “Effect of engineering constraints on charged particle wall heat loads in DEMO”. en. In: *Fusion Engineering and Design* 124 (Nov. 2017), pp. 385–390. ISSN: 09203796. DOI: 10.1016/j.fusengdes.2017.02.077. URL: https://linkinghub.elsevier.com/retrieve/pii/S0920379617301709 (visited on 09/15/2021).

[26] M. Giacomin et al. “Theory-based scaling laws of near and far scrape-off layer widths in single-null L-mode discharges”. In: *Nuclear Fusion* 61.7 (July 2021). Publisher: IOP Publishing, p. 076002. ISSN: 0029-5515, 1741-4326. DOI: 10.1088/1741-4326/abf8f6. URL: https://iopscience.iop.org/article/10.1088/1741-4326/abf8f6 (visited on 07/19/2025).

[27] W. Zholobenko et al. “Filamentary transport in global edge-SOL simulations of ASDEX Upgrade”. en. In: *Nuclear Materials and Energy* 34 (Mar. 2023), p. 101351. ISSN: 23521791. DOI: 10.1016/j.nme.2022.101351. URL: https://linkinghub.elsevier.com/retrieve/pii/S2352179122002320 (visited on 08/02/2023).

[28] S. Peschanyy. “Simulation of Heat Flux to the DEMO First Wall Due to Filamentary Transport in the Far SOL”. In: *IEEE Transactions on Plasma Science* 46.5 (May 2018), pp. 1393–1397. ISSN: 0093-3813, 1939-9375. DOI: 10.1109/TPS.2017.2781191. URL: https://ieeexplore.ieee.org/document/8233124/ (visited on 09/15/2021).

[29] Tiago Pomella Lobo, Sergey Pestchanyi, and Ivan Alessio Maione. “A reduced-order model to estimate first wall particle and heat fluxes for systems codes”. en. In: *Fusion Engineering and Design* 204 (July 2024), p. 114491. ISSN: 09203796. DOI: 10.1016/j.fusengdes.2024.114491. URL: https://linkinghub.elsevier.com/retrieve/pii/S0920379624003442 (visited on 05/21/2024).

[30] R. Arredondo et al. “Preliminary estimates of tritium permeation and retention in the first wall of DEMO due to ion bombardment”. en. In: *Nuclear Materials and Energy* 28 (Sept. 2021), p. 101039. ISSN: 23521791. DOI: 10.1016/j.nme.2021.101039. URL: https://linkinghub.elsevier.com/retrieve/pii/S2352179121001125 (visited on 09/15/2021).

[31] G Holzner et al. “Solute diffusion of hydrogen isotopes in tungsten—a gas loading experiment”. In: *Physica Scripta* T171 (Jan. 2020), p. 014034. ISSN: 0031-8949, 1402-4896. DOI: 10.1088/1402-4896/ab4b42. URL: https://iopscience.iop.org/article/10.1088/1402-4896/ab4b42 (visited on 11/08/2021).

[32] G.A. Esteban et al. “Hydrogen transport and trapping in EUROFER’97”. en. In: *Journal of Nuclear Materials* 367-370 (Aug. 2007), pp. 473–477. ISSN: 00223115. DOI: 10.1016/j.jnucmat.2007.03.114. URL: https://linkinghub.elsevier.com/retrieve/pii/S0022311507004187 (visited on 12/09/2021).

[33] M. Pečovnik et al. “New rate equation model to describe the stabilization of displacement damage by hydrogen atoms during ion irradiation in tungsten”. In: *Nuclear Fusion* 60.3 (Mar. 2020), p. 036024. ISSN: 0029-5515, 1741-4326. DOI: 10.1088/1741-4326/ab680f. URL: https://doi.org/10.1088/1741-4326/ab680f (visited on 09/21/2021).

[34] O.V. Ogorodnikova et al. “Surface modification and deuterium retention in reduced-activation steels under low-energy deuterium plasma exposure. Part I: undamaged steels”. In: *Nuclear Fusion* 57.3 (Mar. 2017), p. 036010. ISSN: 0029-5515, 1741-4326. DOI: 10.1088/1741-4326/57/3/036010. URL: https://iopscience.iop.org/article/10.1088/1741-4326/57/3/036010 (visited on 09/21/2021).

[35] O.V. Ogorodnikova et al. “Surface modification and deuterium retention in reduced-activation steels under low-energy deuterium plasma exposure. Part II: steels pre-damaged with 20 MeV W ions and high heat flux”. In: *Nuclear Fusion* 57.3 (Mar. 2017), p. 036011. ISSN: 0029-5515, 1741-4326. DOI: 10.1088/1741-4326/57/3/036011. URL: https://iopscience.iop.org/article/10.1088/1741-4326/57/3/036011 (visited on 09/21/2021).

[36] M. Beckers et al. “Investigations of the first-wall erosion of DEMO with the CELLSOR code”. en. In: *Nuclear Materials and Energy* 12 (Aug. 2017), pp. 1163–1170. ISSN: 23521791. DOI: 10.1016/j.nme.2017.01.006. URL: https://linkinghub.elsevier.com/retrieve/pii/S235217911630182X (visited on 09/28/2025).

[37] Björn Biltzinger. “Berechnung des Wasserstofftransports in der Wand eines zukünftigen Fusionsreaktors”. German. PhD thesis. Technical University of Munich (TUM), July 2016.